Characterization of Physical, Thermal and Structural Properties of Chromium (VI) Oxide Powder: Impact of Biofield Treatment

Mahendra Kumar Trivedi, Rama Mohan Tallapragada, Alice Branton, Dahryn Trivedi, Gopal Nayak, Omprakash Latiyal, Snehasis Jana

▶ **To cite this version:**

Mahendra Kumar Trivedi, Rama Mohan Tallapragada, Alice Branton, Dahryn Trivedi, Gopal Nayak, et al.. Characterization of Physical, Thermal and Structural Properties of Chromium (VI) Oxide Powder: Impact of Biofield Treatment. Powder Metallurgy & Mining , 2015, 4 (1). hal-01398907

HAL Id: hal-01398907
https://hal.science/hal-01398907

Submitted on 18 Nov 2016

HAL is a multi-disciplinary open access archive for the deposit and dissemination of scientific research documents, whether they are published or not. The documents may come from teaching and research institutions in France or abroad, or from public or private research centers.

L'archive ouverte pluridisciplinaire **HAL**, est destinée au dépôt et à la diffusion de documents scientifiques de niveau recherche, publiés ou non, émanant des établissements d'enseignement et de recherche français ou étrangers, des laboratoires publics ou privés.

Distributed under a Creative Commons Attribution 4.0 International License

Trivedi et al., J Powder Metall Min 2015, 4:1
http://dx.doi.org/10.4172/2168-9806.1000128

Powder Metallurgy & Mining

Research Article Open Access

Characterization of Physical, Thermal and Structural Properties of Chromium (VI) Oxide Powder: Impact of Biofield Treatment

Mahendra Kumar Trivedi[1], Rama Mohan Tallapragada[1], Alice Branton[1], Dahryn Trivedi[1], Gopal Nayak[1], Omprakash Latiyal[2], and Snehasis Jana[2]*

[1]*Trivedi Global Inc, S Eastern Avenue Suite, Henderson, USA*
[2]*Trivedi Science Research Laboratory Pvt. Ltd., Madhya Pradesh, India*

Abstract

Chromium (VI) oxide (CrO_3) has gained extensive attention due to its versatile physical and chemical properties. The objective of the present study was to evaluate the impact of biofield treatment on physical, thermal and structural properties of CrO_3 powder. In this study, CrO_3 powder was divided into two parts i.e. control and treatment. Control part was remained as untreated and treated part received Mr. Trivedi's biofield treatment. Subsequently, control and treated CrO_3 samples were characterized using Thermo gravimetric analysis-differential thermal analysis (TGA-DTA), X-ray diffraction (XRD), and Fourier transform infrared spectroscopy (FT-IR). DTA showed that the melting point of treated CrO_3 was increased upto 212.65°C (T3) as compared to 201.43°C in control. In addition, the latent heat of fusion was reduced upto 51.70% in treated CrO_3 as compared to control. TGA showed the maximum thermal decomposition temperature (T_{max}) around 330°C, was increased upto 340.12°C in treated CrO_3 sample. XRD data revealed that lattice parameter and unit cell volume of treated CrO_3 samples were reduced by 0.25 and 0.92% respectively, whereas density was increased by 0.93% in treated CrO_3 sample as compared to control. The crystallite size of treated CrO_3 was increased from 46.77 nm (control) to 60.13 nm after biofield treatment. FT-IR spectra showed the absorption peaks corresponding to Cr=O at 906 and 944 cm^{-1} in control, which were increased to 919 and 949 cm^{-1} in treated CrO_3 after biofield treatment. Overall, these results suggest that biofield treatment has substantially altered the physical, thermal and structural properties of CrO_3 powder.

Keywords: Biofield treatment; Chromium (VI) oxide powder; X-Ray diffraction; Fourier Transform Infrared Spectroscopy; TGA-DTA

Introduction

Chromium oxides gain significant attention due to their diverse technological application in various industries. Chromium based oxides are used in various chemical reactions due to their wide range of oxidations states, it includes CrO_2, Cr_2O_3, Cr_2O_5 and CrO_3 etc [1]. Out of these, chromium oxides, CrO_3 is an important compound for automobile industries due to its high corrosion resistance properties. In these industries, CrO_3 is used for plating the chromium on car body and other auto components. In addition, it is a strong oxidising agent, which enables it to be used in various pharmaceutical and chemical industries [2,3]. It is also reported that Cr (VI) complexes exhibit the antibacterial activity against *Pseudomonas aeruginosa* bacteria [4]. In crystal structure of CrO_3, its molecules form the chains of CrO_4 tetrahedra, which are linked at corner oxygen [5]. Furthermore, the crystal structure parameters such as lattice parameter, unit cell volume of CrO_3 play a crucial role in modulating its chemical and physical properties. Thus, based on the above applications of CrO_3 powder, authors planned to investigate an approach that could modify its physical, thermal and structural properties.

In physics, energy is a property of object which can be transferred to other objects, but it neither be created nor be destroyed. Albert Einstein proposed the relationship between mass and energy i.e. $E=mc^2$ [6]. This energy can be transferred through various processes such as thermal, chemical, kinetic, nuclear etc. Similarly, human nervous system consists of neurons, which have the ability to transmit information in the form of electrical signals [7-9]. Due to this, a human has ability to harness the energy from environment/universe and can transmit into any object (living or non-living) around the Globe. The object(s) always receive the energy and responded into useful way that is called biofield energy. This process is termed as biofield treatment. Mr. Trivedi's unique biofield treatment (The Trivedi Effect®) is known to alter the physical, structural and atomic characteristic in various metals [10-12] and ceramics [13]. Additionally, the impact of biofield treatment has been studied extensively in various fields such as microbiology [14,15], biotechnology [16,17], and agriculture [18-20]. Moreover, biofield treatment has significantly altered the particle size and crystallite size in zinc powder upto six and two folds, respectively [21]. In addition, it has substantially altered the unit cell volume and molecular weight in vanadium pentoxide [13]. Thus, based on the literature and excellent outcomes of biofield treatment, authors interested to investigate the effect of biofield treatment on physical, thermal and structural properties of CrO_3 powder.

Materials and Methods

The CrO_3 powder was purchased from Sigma Aldrich, India. The sample was equally divided into two parts, considered as control and treated. Treated group was in sealed pack and handed over to Mr. Trivedi for biofield treatment under laboratory condition. Mr. Trivedi provided the biofield treatment through his energy transmission process to the treated group without touching the sample. The control and treated samples were characterized using Thermo gravimetric

***Corresponding author:** Snehasis Jana, Trivedi Science Research Laboratory Pvt. Ltd., Hall-A, Chinar Mega Mall, Chinar Fortune City, Hoshangabad Rd, Bhopal-462026, Madhya Pradesh, India, Tel: +91-755-6660006; E-mail: publication@trivedisrl.com

Received August 10, 2015; **Accepted** August 11, 2015; **Published** August 18, 2015

Citation: Trivedi MK, Tallapragada RM, Branton A, Trivedi D, Nayak G, et al. (2015) Characterization of Physical, Thermal and Structural Properties of Chromium (VI) Oxide Powder: Impact of Biofield Treatment. J Powder Metall Min 4: 128. doi:10.4172/2168-9806.1000128

Copyright: © 2015 Trivedi MK, et al. This is an open-access article distributed under the terms of the Creative Commons Attribution License, which permits unrestricted use, distribution, and reproduction in any medium, provided the original author and source are credited.

analysis-differential thermal analysis (TGA-DTA), X-ray diffraction (XRD), and Fourier transform infrared spectroscopy (FT-IR).

Thermo Gravimetric Analysis-Differential Thermal Analysis (TGA-DTA)

Thermal analysis of control and treated CrO_3 was analysed using Mettler Toledo simultaneous TGA and Differential thermal analyser (DTA). The samples were heated from room temperature to 400°C with a heating rate of 5°C/min under air atmosphere. From DTA, melting point and latent heat of fusion (ΔH) were computed using integral area under peaks. Thermal decomposition temperature (T_{max}) was recorded from TGA curve. Percent change in melting point was calculated using following equation:

$$\% \text{ change in Melting Point} = \left[\frac{T_{Treated} - T_{Control}}{T_{Control}}\right] \times 100$$

Where, $T_{Control}$ and $T_{Treated}$ are the melting point of control and treated samples, respectively.

Similarly, percent change in ΔH and T_{max} were calculated.

X-ray Diffraction study (XRD)

XRD analysis of control and treated CrO_3 powder was carried out on Phillips, Holland PW 1710 X-ray diffractometer system, which had a copper anode with nickel filter. The radiation of wavelength used by the XRD system was 1.54056Å. The data obtained from this XRD were in the form of a chart of 2θ vs. intensity and a detailed table containing peak intensity counts, d value (Å), peak width (θ°), relative intensity (%) etc. Additionally, PowderX software was used to calculate lattice parameter and unit cell volume of CrO_3 powder samples. Weight of the unit cell was calculated as, molecular weight multiplied by the number of atoms present in a unit cell.

The crystallite size (G) was calculated by using formula:

$G=k\lambda/(b\text{Cos}\theta)$,

Here, λ is the wavelength of radiation used, b is full width half maximum (FWHM) and k is the equipment constant (0.94). Furthermore, the percent change in the lattice parameter was calculated using following equation:

$$\% \text{ change in lattice parameter} = \left[\frac{A_{Treated} - A_{Control}}{A_{Control}}\right] \times 100$$

Where $A_{Control}$ and $A_{Treated}$ are the lattice parameter of treated and control samples respectively. Similarly, the percent change in all other parameters such as unit cell volume, density, molecular weight, and crystallite size were calculated.

Fourier Transform Infrared Spectroscopy (FT-IR)

FT-IR spectroscopic analysis was carried out to evaluate the impact of biofield treatment at atomic and molecular level like bond strength, stability, and rigidity of structure etc. [22]. FT-IR analysis of control and treated CrO_3 samples was performed on Shimadzu, Fourier transform infrared (FT-IR) spectrometer with frequency range of 300-4000 cm^{-1} was used.

Results and Discussion

Thermo Gravimetric Analysis-Differential Thermal Analysis (TGA-DTA)

Thermal analysis of control and treated CrO_3 samples was performed using TGA-DTA and results are presented in Table 1. DTA result showed that melting point of control sample was 201.43°C in control, however it was changed to 204.28°C, 204.24°C, 212.65°C and 200.88°C in treated CrO_3 samples T1, T2, T3 and T4, respectively. It indicated that melting point was increased by 1.41, 1.40, and 5.57% in T1, T2, and T3, respectively, whereas a slight change (-0.27%) was observed in T4, as compared to control. Furthermore, data also showed that the simultaneous DTA (SDTA) integral area (denoted as negative value) at melting point was 235.53, 252.69, 235.13, 414.03, and 142.22 s °C in control, T1, T2, T3 and T4, respectively (Table 1). Further, SDTA integral values were used to compute the latent heat of fusion of control and treated CrO_3 samples. The latent heat of fusion (ΔH) was 486.87J/g in control, whereas it was changed to 507.37, 274.04, 235.15, and 433.09 J/g in T1, T2, T3 and T4 respectively. Thus, data suggest that ΔH was increased by 4.21% in T1, however it was decreased by 43.71, 51.70, and 11.05% in T2, T3 and T4, respectively as compared to control. The melting point is fundamentally related with the kinetic energy and thermal vibration of the molecules, whereas latent heat of fusion is relates with the potential energy of molecules. Thus, the changes in melting point and ΔH after biofield treatment indicated that biofield treatment probably altered the kinetic and potential energy of the CrO_3 molecules. It is assumed the bio field treatment might transfer the energy to treated sample, which probably altered the internal energy of the molecules. Besides, the thermal decomposition temperature (T_{max}) was observed at 330°C in control and it was increased to 335, 336.98, 333.4, and 340.1°C in T1, T2, T3 and T4 respectively. It could be due to decomposition of CrO_3 to Cr_2O_5 and Cr_3O_8 It is reported that in thermal decomposition process of CrO_3, first converts to Cr_2O_5 followed by Cr_3O_8 [23]. Further, data suggest that T_{max} was increased by 1.52, 2.12, 1.02, and 3.07% in T1, T2, T3 and T4, respectively as compared to control. It could be due to increase in thermal stability of treated CrO_3 samples after biofield treatment. In this process, samples lost around 13.28, 14.49, 82.57, 10.48, and 6.03% of its weight in control, T1, T2, T3, and T4, respectively. Recently, it was reported that biofield treatment has altered the percent weight loss in treated lead and tin powders [12]. The percent of weight loss of CrO_3 powder sample was higher in T1, T2, and T3 but lesser in T4, as compared to control. It could be due to change in intermolecular interaction and thermal stability in treated CrO_3 after biofield treatment. Hence, TGA-DTA study revealed that biofield treatment has significantly altered the thermal properties of CrO_3 powder.

X-ray Diffraction study (XRD)

XRD pattern of control and treated CrO_3 samples are presented in Figure 1. The control sample peaks in XRD pattern were observed at 2θ=21.33°, 26.01°, 26.42°, 31.16°, 37.53°, 37.97°, and 40.03° which were

Parameters	Control	T1	T2	T3	T4
Melting point (°C)	201.43	204.28	204.24	212.65	200.88
% change		1.41	1.4	5.57	-0.27
SDTA integral area at melting point (s°C)	-235.53	-252.69	-235.13	-414.03	-142.22
Latent heat of fusion, ΔH (J/g)	486.87	507.37	274.04	235.15	433.09
% change		4.21	-43.71	-51.7	-11.05
Decomposition Temp, Tmax (°C)	330	335	336.98	333.36	340.12
Percent change		1.52	2.12	1.02	3.07
Percent weight loss at Tmax	-13.28	-14.49	-82.57	-10.48	-6.03

Table 1: TGA-DTA analysis of chromium (VI) oxide powder.

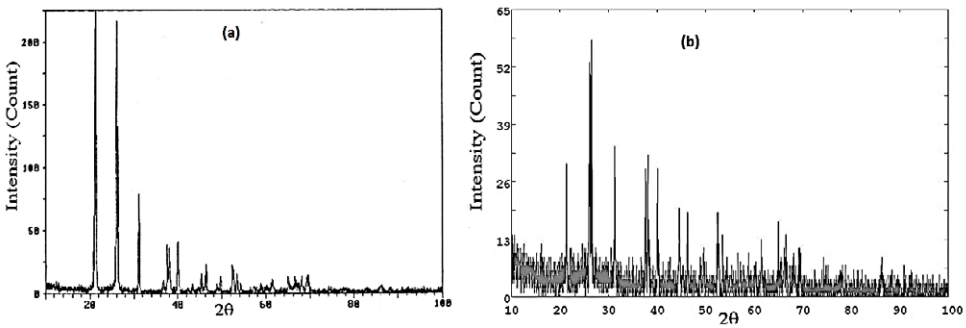

Figure 1: XRD pattern of chromium (VI) oxide powder. (a) Control and (b) Treated.

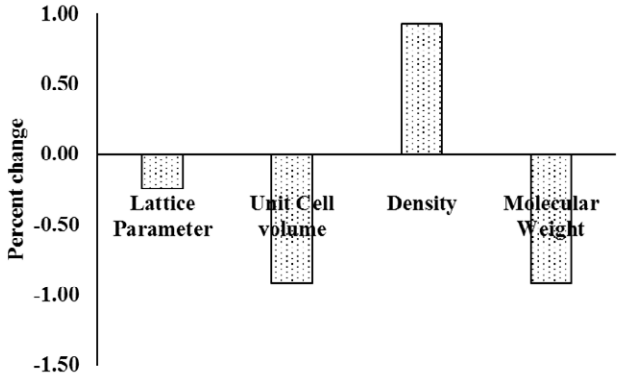

Figure 2: Effect of biofield treatment on lattice parameter, unit cell volume, density, and molecular weight of treated chromium (VI) oxide powder as compared to control.

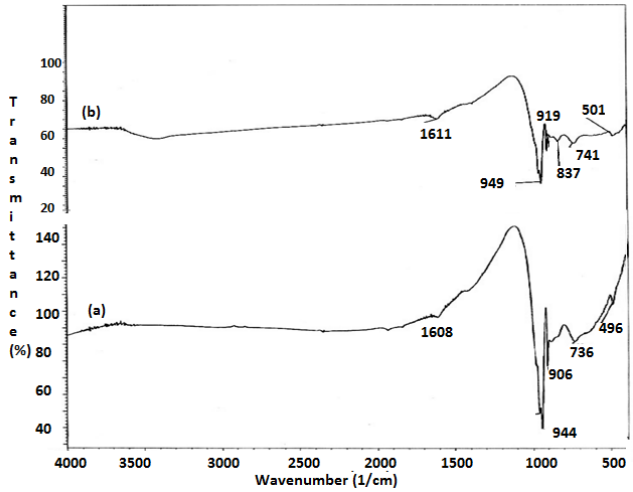

Figure 3: FT-IR spectrum of chromium (VI) oxide powder. (a) Control and (b) Treated.

supported by literature data of CrO_3 [24]. However, XRD of treated CrO_3 sample exhibited peaks at 2θ=21.39°, 26.13°, 26.51°, 31.32°, 37.63°, and 38.11°. The intense peaks in XRD pattern of control and treated CrO_3 samples suggested its crystalline nature. Further, the crystal structure parameter such as lattice parameter, and unit cell volume were calculated using PowderX software and their percent change with respect to control are presented in Figure 2. Data showed that the lattice parameter and unit cell volume was reduced by 0.25 and 0.92%, respectively as compared to control. The change in unit cell volume can be considered as volumetric strain. Herein, negative volumetric strain found in treated CrO_3 indicated that biofield treatment possibly induced compressive stress along the lattice parameter "a" that led to reduced unit cell volume in treated sample. Recently, alteration in unit cell volume and lattice parameter in zinc oxide, iron oxide and copper oxides using biofield treatment was reported by our group [25]. In addition, the density of treated CrO_3 was increased by 0.93% and molecular weight was reduced by 0.92% as compared to control. It could be possible if number of protons and neutron altered after biofield treatment. Thus, it is hypothesized that a weak reversible nuclear level reaction including neutrons-protons and neutrinos might occur in treated CrO_3 powders after biofield treatment [26]. Besides, the crystallite size was calculated using Scherrer formula is presented in Table 2. Data showed that crystallite size was 46.77 nm in control, whereas it was increased to 60.13 nm in treated sample. It suggested that crystallite size was increased by 28.57% as compared to control. Previously, our group reported that biofield treatment has increase the crystallite size in silicon dioxide [27], silicon carbide [28] and antimony

Crystallite Size (nm)		% change in
Control	Treated	Crystallite size
46.77	60.13	28.57

Table 2: Effect of biofield treatment on crystallite size chromium (VI) oxide powder.

[29]. Furthermore, in order to increase the crystallite size, sufficient amount of energy is required to move the crystallite boundaries. Thus, it is hypothesised that the energy required for this process might be transferred through biofield treatment and that might be responsible for increase in crystallite size. Hence, XRD data revealed that biofield treatment has altered the physical and structural properties of CrO_3 powder.

Fourier Transform Infrared Spectroscopy (FT-IR)

FT-IR spectrum of control and treated are shown in Figure 3. IR spectra exhibited the absorption peaks at 496, 736, 906, and 944 cm^{-1} in control, whereas these peaks were shifted to higher wavenumber i.e. 501, 741, 919, and 949 cm^{-1} in treated CrO_3 spectra. The peaks at 906 and 944 cm^{-1} in control and 919 and 949 cm^{-1} in treated CrO_3 can be attributed to chromyl (Cr=O) vibrations [30]. The wavenumber observed in IR spectra is directly proportional to bond force constant. Thus it is assumed that the increase in wave number for Cr =O vibration could be due to increase in bond force constant after biofield treatment.

In our previous study on iron oxide, biofield treatment had altered the bond strength of Fe-O bond [25]. Thus, it is hypothesized that the energy transferred through biofield treatment probably enhanced the Cr=O bond strength in treated CrO_3 molecules, which may lead to increase bond force constant, thus increase the wavenumber. In addition, the increase in Cr=O bond strength could increase the stability of CrO_3 molecules. It is also supported by increase in thermal stability of treated CrO_3 after biofield treatment.

Conclusion

The thermal analysis of CrO_3 using TGA-DTA revealed that biofield treatment has altered the melting point, ΔH, and T_{max}. The melting point was increased upto 5.57% in treated CrO_3, whereas ΔH was reduced upto 51.70% in treated as compared to control. It is assumed that biofield treatment probably altered the internal energy of treated CrO_3 samples, which may lead to alter the melting point and ΔH. In addition, T_{max} was slightly increased up to 3.077% as compared to control. Besides, XRD data exhibited the alteration in lattice parameter, unit cell volume, density, and molecular weight in treated CrO_3 as compared to control. The crystallite size of treated CrO_3 sample was increased by 28.57% as compared to control. It may be due to movement of crystallite boundaries through biofield energy, which probably transferred via biofield treatment. FT-IR spectra revealed that the absorption peaks were shifted from 906 and 944 cm^{-1} (control) to higher wavenumber i.e. 919 and 949 cm^{-1} in treated CrO_3 sample. It could be due to increase of bond force constant of Cr=O bond after biofield treatment. Overall, study results suggest that biofield treatment has significantly altered the thermal, physical and structural properties of CrO_3 powder. It is also assumed that biofield treated CrO_3 could be useful for chrome plating applications in automobile industries.

Acknowledgement

Authors gratefully acknowledged to Dr. Cheng Dong of NLSC, Institute of Physics, and Chinese academy of Sciences for providing the facilities to use PowderX software for analyzing XRD data. Authors also would like to thank Trivedi Science, Trivedi master wellness and Trivedi testimonials for their support during the work.

References

1. Zhai HJ, Li S, Dixon DA, Wang LS (2008) Probing the electronic and structural properties of chromium oxide clusters $(CrO_3)_n^-$ and $(CrO_3)_n$ (n=1-5): Photoelectron spectroscopy and density functional calculations. J Am Chem Soc 130: 5167-5177.
2. Zhao M, Li J, Song Z, Desmond R, Tschaen DM et al. (1998) A novel chromium trioxide catalyzed oxidation of primary alcohols to the carboxylic acids. Tetrahedron Lett 39: 5323-5326.
3. Corey EJ, Link JO, Shao Y (1992) Two effective procedures for the synthesis of trichloromethyl ketones, useful precursors of chiral α-amino and α-hydroxy acids. Tetrahedron Lett 33: 3435-3438.
4. Jaswal VS, Arora AK, Singh J, Kinger M, Gupta VD (2014) Synthesis and characterization of chromium oxide nanoparticles. Orient J Chem 30: 559-566.
5. Stephens JS, Cruickshank DWJ (1970) The crystal structure of $(CrO_3)_\infty$. Acta Cryst B26: 222-226.
6. Einstein A (1905) Does the inertia of a body depend upon its energy-content. Annalen der Physik 18: 639-641.
7. Becker RO, Selden G (1985) The body electric: Electromagnetism and the foundation of life. William Morrow and Company, New York City, USA.
8. Barnes RB (1963) Thermography of the human body. Science 140: 870-877.
9. Born M (1971) The Born-Einstein Letters (1stedn). Walker and Company, New York.
10. Trivedi MK, Patil S, Tallapragada RM (2012) Thought intervention through bio field changing metal powder characteristics experiments on powder characteristics at a PM plant. Future Control and Automation LNEE 173: 247-252.
11. Trivedi MK, Patil S, Tallapragada RM (2015) Effect of biofield treatment on the physical and thermal characteristics of aluminium powders. Ind Eng Manage 4: 151.
12. Trivedi MK, Patil S, Tallapragada RM (2013) Effect of biofield treatment on the physical and thermal characteristics of silicon, tin and lead powders. J Material Sci Eng 2: 125.
13. Trivedi MK, Patil S, Tallapragada RM (2013) Effect of biofield treatment on the physical and thermal characteristics of vanadium pentoxide powder. J Material Sci Eng S11: 001.
14. Trivedi MK, Patil S, Shettigar H, Gangwar M, Jana S (2015) Antimicrobial sensitivity pattern of *Pseudomonas fluorescens* after biofield treatment. J Infect Dis Ther 3: 222.
15. Trivedi MK, Patil S, Shettigar H, Bairwa K, Jana S (2015) Phenotypic and biotypic characterization of *Klebsiella oxytoca*: An impact of biofield treatment. J Microb Biochem Technol 7: 203-206.
16. Patil SA, Nayak GB, Barve SS, Tembe RP, Khan RR (2012) Impact of biofield treatment on growth and anatomical characteristics of *Pogostemon cablin* (Benth). Biotechnology 11: 154-162.
17. Altekar N, Nayak G (2015) Effect of biofield treatment on plant growth and adaptation. J Environ Health Sci 1: 1-9.
18. Shinde V, Sances F, Patil S, Spence A (2012) Impact of biofield treatment on growth and yield of lettuce and tomato. Aust J Basic and Appl Sci 6: 100-105.
19. Lenssen AW (2013) Biofield and fungicide seed treatment influences on soybean productivity, seed quality and weed community. Agricultural Journal 8: 138-143.
20. Sances F, Flora E, Patil S, Spence A, Shinde V (2013) Impact of biofield treatment on ginseng and organic blueberry yield. Agrivita J Agric Sci 35.
21. Trivedi MK, Tallapragada RM (2008) A transcendental to changing metal powder characteristics. Met Powder Rep 63: 22-28.
22. Pavia DL, Lampman GM, Kriz GS (2001) Introduction to spectroscopy (3rdedn) Thomson Learning, Singapore.
23. Fouad NE (1996) Non-isorhermal kinetics of CrO_3 decomposition pathways in air. J Therm Anal 46: 1271-1282.
24. Sajadi SAA, Khaleghian M (2014) Study of thermal behavior of CrO3 using TG and DSC. J Therm Anal Calorim 116: 915-921.
25. Trivedi MK, Nayak G, Patil S, Tallapragada RM, Latiyal O (2015) Studies of the atomic and crystalline characteristics of ceramic oxide nano powders after bio field treatment. Ind Eng Manage 4: 161.
26. Narlikar JV (1993) Introduction to cosmology (2nd edn) Jones and Bartlett Inc., Cambridge University Press.
27. Trivedi MK, Patil S, Tallapragada RM (2014) Atomic, crystalline and powder characteristics of treated zirconia and silica powders. J Material Sci Eng 3: 144.
28. Trivedi MK, Nayak G, Tallapragada RM, Patil S, Latiyal O, et al. (2015) Effect of biofield treatment on structural and morphological properties of silicon carbide. J Powder Metall Min 4:1.
29. Dhabade VV, Tallapragada RM, Trivedi MK (2009) Effect of external energy on atomic, crystalline and powder characteristics of antimony and bismuth powders. Bull Mater Sci 32: 471-479.
30. Weckhuysen BM, Wachs IE, Schoonheydt RA (1996) Surface chemistry and spectroscopy of chromium in inorganic oxides. Chem Rev 96: 3327-3349.

Citation: Trivedi MK, Tallapragada RM, Branton A, Trivedi D, Nayak G, et al. (2015) Characterization of Physical, Thermal and Structural Properties of Chromium (VI) Oxide Powder: Impact of Biofield Treatment. J Powder Metall Min 4: 128. doi:10.4172/2168-9806.1000128